

## **Application of radar-measured rain data in hydrological processes modelling during the intensified observation period of HUBEX**

**LILIANG REN, CHUNHONG LI & MEIRONG WANG**

*Department of Hydrology and Water Resources, Hohai University, No. 1 Xikang Road, Nanjing 210098, China*

[rl@hhu.edu.cn](mailto:rl@hhu.edu.cn)

**ABSTRACT** Raster flow vectors and watershed delineation were generated from the DEM for the upper area of Huangnizhuang station in the Shihe catchment intensified observation field for the HUBEX/GAME project. The Xinanjiang model was then applied for runoff production in each grid element where rain data measured by weather radar at Fuyang station were used as the input of the hydrological model after correction. Those elements are connected by flow vectors with the outlet of drainage catchment, in which runoff is routed by the Muskingum method from each grid element to the outlet. The Nash-Sutcliffe model efficiency coefficient is up to 92.41% from 31 May to 3 August 1998. The index of model efficiency improvement is 51.22% if compared with the case where raingauge data were used. This shows that radar-measured data are superior to raingauge data as the input of hydrological modelling.

**Key words** catchment; digital elevation model; hydrological processes; radar; raster; Xinanjiang model

### **INTRODUCTION**

Topography is of great importance to the description, quantification, and interpretation of land surface processes, such as water and energy fluxes, evapotranspiration and soil erosion (Beven, 1989; Moore *et al.*, 1991). Topography varies from one location to another and topographical variability affects the apparent slope, flow path, land cover and soil formation. Moreover, topography is easily available earth surface information. Extracting topographical information for a watershed by traditional and manual operation might be tedious, time-consuming and error-prone. Research over the past decades has demonstrated the feasibility of extracting topographical information directly from raster-based digital elevation models (DEMs) (Doyle, 1978; O'Callaghan & Mark, 1984; Jenson & Dominique, 1988). In the field of hydrology and water resources, automatic evaluation of DEMs has mainly focused on watershed segmentation, definition of drainage divides and identification of river networks. This automatic extraction of network and subwatershed properties from the DEM represents a convenient and rapid way to parameterize a watershed (Garbrecht & Campbell, 1997).

The development of computer science and digital techniques such as DEMs provide a solid technical foundation for the revolution of hydrological modelling. The spatial distribution of land surface characteristics, such as topography, land-cover, soil, watershed divide, drainage network, catchment area, could be expressed digitally, so as

to avoid using the conventional manual method. Thus the digital hydrological model emerges. This digital hydrological model is a modern, physically-based modelling technique containing a large amount of information. It is a DEM-based distributed model, and the combination of grid-based runoff generation model with streamflow routing model. In this study, the Xinanjiang model (Zhao, 1992) is applied for the development of digital rainfall-runoff model in each grid element that is generated and numbered automatically by the Digital Elevation Drainage Network Model (DEDNM; Martz & Garbrecht, 1992).

Techniques for solving hydrological problems are borrowed from several disciplines such as mathematics, statistics, operation research, computer science and information theory. Based on solution techniques, hydrology can be subdivided into different branches. Thus digital hydrology results from the intersection of computer science and hydrology. Intrinsically, being digital connotes being discrete in space or in time. In such a sense, it seems to us that digital hydrology focuses our attention on the spatial separation of a catchment as gridded cells or subcatchments, and the temporal discretization of hydrological processes within each cell or each subcatchment. Therefore, state values and instantaneous values of hydrological elements could be modelled at any site and at any time step, so as to show the whole hydrological process. In order to attain this goal, rainfall, as the input to hydrological model, is of great importance, especially for short-duration flood hydrograph modelling according to the past experience of rainfall-runoff modelling. The spatial variability of precipitation is very significant for runoff computation. Radar-based rain data have an advantage over highly spatial and temporal resolutions. Such an advantage may be fully and completely utilized in the grid-based hydrological model. In addition, the spatial and temporal distributions of state variables, such as soil tension water at any cell within the catchment at any time step, could be obtained by the model.

A catchment may be partitioned spatially as grid elements by the DEDNM. Thus a grid element on the ground within the catchment matches the atmospheric input, such as precipitation and evapotranspiration. It is of theoretical significance and of practical value to apply radar-measured rain data to digital hydrological modelling.

## **STUDY AREA AND DATA**

The Shihe catchment within 31.2–32.3°N latitude and 115.25–115.75°E longitude is selected for the case study. The Huangnizhuang station is the outlet of that catchment with an area of 805 km<sup>2</sup>. The Shihe River is the first-order southern tributary of the Huaihe River basin. There exists a highly mountainous area where the streamflow goes very fast. The Shihe catchment is selected as the intensified observation field for the HUBEX/GAME project supported financially from the National Natural Science Foundation of China during the ninth Five Year Plan.

DEM data were obtained from National Geophysical Data Center, USA, viz. Global Land One-kilometre Base Elevation (GLOBE) data. On the basis of DEM pre-processing, the steepest down slope path method is applied to the determination of flow vectors on each grid. Figure 1 shows the visual flow vectors over the Shihe catchment.

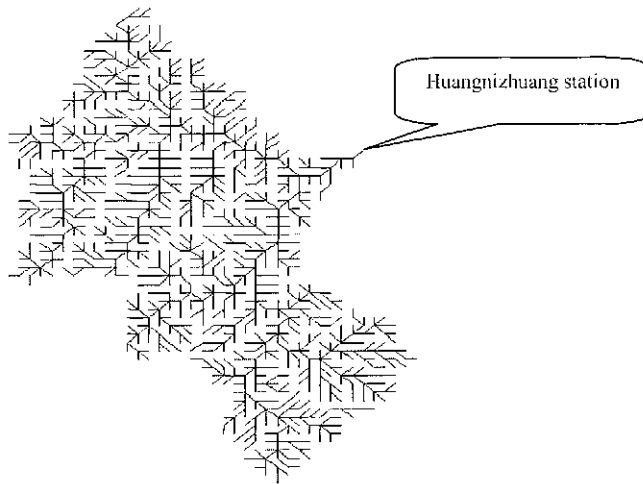


**Fig. 1** Raster-based flow vectors in the upper area of Huangnizhuang station in the Shihe catchment, produced by the steepest descent method.

Radar reflectivity data were obtained from a C-band weather radar device with 5 cm of wavelength. It lies at 32.93°N latitude, 115.83°E longitude in Fuyang, Anhui Province. Fuyang radar scans a radius of about 250 km, within which the Shihe catchment lies. Radar reflectivity data are continuously observed by the volume scanning method. The radar scans one volume per 10 min with 1 km of spatial resolution. Every volume data set has 14–16 PPI. All PPI data were filtered and averaged within 1 h, after eliminating noise and correcting obstruction from cluster (Liu *et al.*, 2000).

## METHODS

### Determination of raster flow vectors

The Digital Elevation Drainage Network Model (DEDNM) developed by Martz & Garbrecht (1992), or so-called TOPographical PARAMeterization (TOPAZ), is applied in this presentation for assigning flow-vector directions over flat and depressional areas of the DEM, and for identifying stream network and watershed divides. The algorithm of the DEDNM is introduced very briefly as follows.

Depressions are sinks at the bottom of which the drainage network terminates. They are probably real storage volumes such as reservoirs, ponds, or artefacts of the horizontal and vertical DEM resolution, DEM generation method, and elevation data truncation. The program is able to distinguish between two types of depressions: sink-depressions and impoundment-depressions. Sink-depressions are caused by a group of raster cells at lower elevation than the surrounding landscape. Impoundment-depressions are caused by a narrow band of raster cells of higher elevation across drainage paths, similar to an obstruction or dam across a stream. In the latter situation,

the program can breach the obstruction in the downstream direction of the drainage path, so as to let water pass it. Any remaining depression after breaching is regarded as a sink-depression, which is treated in the conventional manner by raising the elevations within the depression to the elevation of its lowest (breached) overflow.

The flat area refers to a group of raster cells with equal values of elevation and indeterminate drainage direction. The flat surface is inherent to the DEM, or comes from the above depression filling. A relief imposition algorithm proposed by Martz & Garbrecht (1992) is adopted for flow-vector designation over the flat area, which takes topographical characteristics around the flat area into account.

The program scans each cell of rectified DEM, and determines the direction of the steepest downward slope to an adjacent cell. This method is termed the D8 (deterministic eight-neighbours) method by Fairfield & Leymarie (1991). The final result is a new raster array containing flow vectors for all grid cells.

The row and column coordinates of a grid cell close to the watershed outlet must be given. With this information, the program displays a portion of catchment-area values around the initial outlet point to the monitor. On this display large upslope catchment-area values identify the channel network, and the user can then modify the watershed outlet coordinates. This updated value is used as the starting point to define the entire upstream drainage area by concurrently scanning flow vectors and watershed grids. The final result of this stage is a raster array defining cells inside and outside the watershed.

## Development of hydrological model

The Xinanjiang model (Zhao, 1992) is characterized by the concept of runoff formation on repletion of storage, i.e. runoff is not produced until the soil moisture content of the aeration zone reaches field capacity, and thereafter runoff equals the rainfall excess without further loss. That concept could be understandable when applied to a point. The tension water storage capacity curve was introduced by Zhao in the 1960s while applied to a catchment. In this research, the parabolic curve is applied to each grid element.

Three kinds of spatially heterogeneous distributions are taken into consideration in the Xinanjiang model: (a) uneven distribution of tension water storage capacity throughout the subcatchment is expressed by a parabolic curve for partial-area runoff generation; (b) non-uniform distribution of free water storage capacity over partial area where runoff has been produced, is expressed also in terms of a parabolic curve for separation of runoff into surface flow, interflow and groundwater flow; and (c) the amount of free water storage is represented by the structure of linear reservoir for the sake of different velocities of different runoff components.

The Xinanjiang model (Zhao, 1992) is applied for runoff production in each grid element where rain data measured by radar at Fuyang station (Liu *et al.*, 2000) are used as the input of the hydrological model. The time step is taken as 1 h for radar-measured rain data. Hence, the time step is 1 h for the computation of the Xinanjiang model. Those elements are connected by flow vectors (as shown in Fig. 1) with the outlet of drainage catchment where runoff is routed by the successive sub-reaches of the

**Table 1** Number of sub-reaches and channel length between the outlet (Huangnizhuang station) and each grid element within the Shihc catchment.

Grid ID	Length (m)	No. of sub-reaches	Grid ID	Length (m)	No. of sub-reaches
1	35222.4	10	11	32785	9
2	36084.3	10	...	...	...
3	34003.7	9	...	...	...
4	34865.6	10	...	...	...
5	35727.5	10	1078	42979.5	12
6	32785	9	1079	43841.4	12
7	32428.1	9	1080	43841.4	12
8	32785	9	1081	44198.2	12
9	33646.9	9	1082	44555.1	12
10	32785	9	1083	45060.1	13

Muskingum method from each grid element to the outlet, according to the channel length (see Table 1) between each grid and the outlet. The length is obtained by summing up the length of gridded cells along the raster-based flow vectors as shown in Fig. 1. Assuming that runoff flows at the speed of  $1 \text{ m s}^{-1}$ , the number of successive sub-reaches in the Muskingum method is obtained by the length divided by 3600 (see Table 1), since the time step is taken as 1 h.

## RESULT ANALYSIS

As shown in Figs 2 and 3, the Nash-Sutcliffe model efficiency coefficient (Nash & Sutcliffe, 1970) is up to 92.41% from 31 May to 3 August 1998, and 85.64, 86.62, 92.57 and 83.91%, respectively, for the first, second, third and fourth flood event during the whole computational period.

The comparison of model efficiency coefficients was made as radar-measured and rain gauge data were used in simulating hourly hydrograph at Huangnizhuang

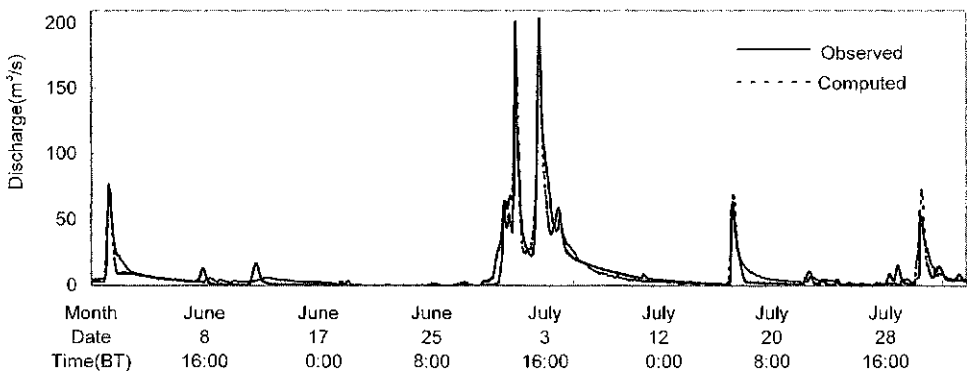


**Fig. 2** Comparison between observed and computed discharges at Huangnizhuang station from 31 May until 3 August 1998, with 92.41% of model efficiency coefficient.

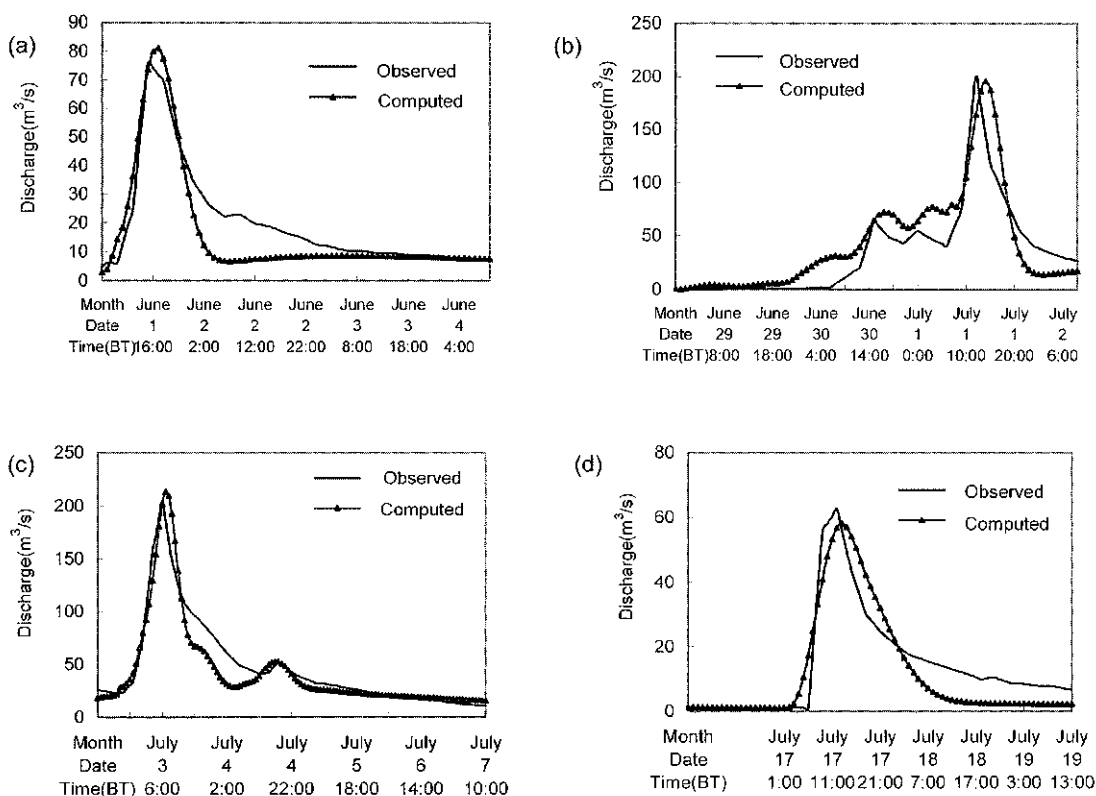


**Fig. 3** Comparison between observed and computed discharges at Huangnizhuang station from June to July in 1998, with 85.64, 86.62, 92.57 and 83.91% of model efficiency coefficient, respectively, for the first, second, third and fourth flood event as shown in (a), (b), (c), (d).

**Table 2** Comparison of model efficiency coefficients as radar-measured and raingauge data were used in simulating hourly discharge hydrograph at Huangnizhuang station in the Shihe catchment, respectively.

Computational period	Model efficiency coefficient $R$ (%)		Improvement index (%) $r = (R_2 - R_1)/(1 - R_1)$
	Raingauge data used ( $R_1$ )	Radar data used ( $R_2$ )	
First flood event	77.81	85.64	35.29
Second flood event	81.53	86.62	27.56
Third flood event	75.73	92.57	69.39
Fourth flood event	73.51	83.91	39.26
During the whole period from 31 May to 3 Aug.	84.44	92.41	51.22

station in the Shihe catchment, respectively. It is seen from Table 2 that the values of model efficiency coefficient  $R$  are higher as radar-measured data were used both for the whole computational period from 31 May to 3 August and for four flood events.

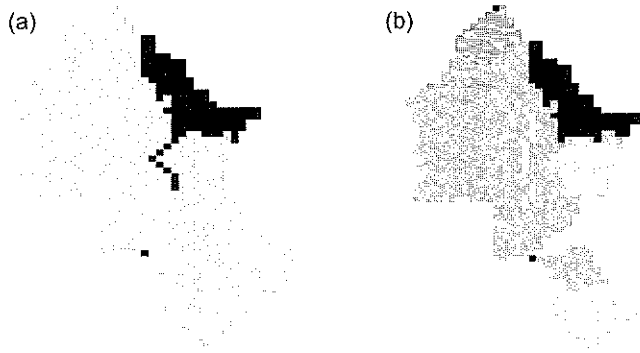


**Fig. 4** Spatial distributions of (a) runoff depth and (b) soil tension water storage in each grid cell at 17:00 h (BT) on 19 June, 1998 (the darker indicates the larger value of runoff or soil water).

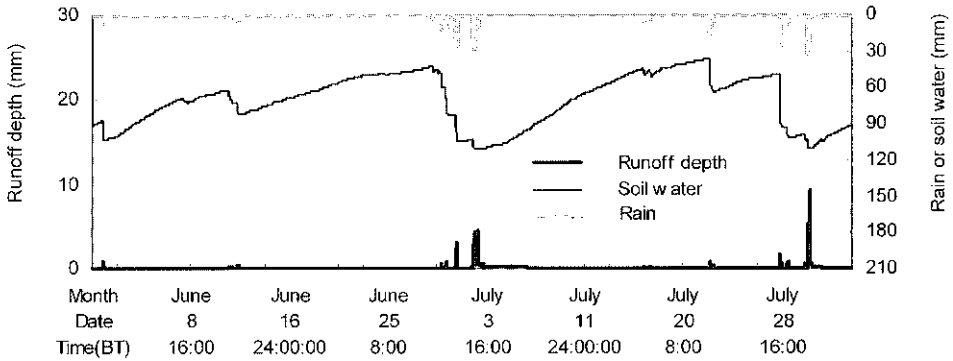


**Fig. 5** Time series of rain, runoff depth, and soil tension water storage in the tenth grid cell within the Shihe catchment.

Therefore, the index of model efficiency improvement of Model 2 (radar-measured rain data being used) over Model 1 (raingauge data being used), expressed by  $r$ , arrives at 51.22% during the whole computational period, and is positive from 27.56% to 69.39% for four flood events. This shows that radar-measured data are superior to raingauge data as the input of hydrological modelling.

In addition, spatial distribution and time series of state variables, such as rain, runoff depth, soil tension water storage on each grid, could also be obtained from the Xinjiang model. It can be seen from Fig. 4 that more runoff is generated where there is more soil tension water storage. In Fig. 5, runoff depth is temporally in agreement with rain and soil tension water storage.

### CONCLUSIONS

The name of digital hydrology matches the reality, only as a catchment is spatially divided into grid elements and the whole hydrological process is recognized at any

space/time scale. It is well known that rainfall plays an important part in hydrological process modelling. The spatial variability of precipitation is very significant for runoff computation. Radar can meet the requirement of hydrological modelling, which offers rain data with high spatial and temporal resolutions. Such an advantage may be fully and completely utilized in the grid-based hydrological model.

After a catchment is segmented spatially as grid elements by the DEDNM, a grid element on the ground within the catchment matches the atmospheric input, such as precipitation and evapotranspiration. The grid-based hydrological model provides a good platform for runoff computation, in which radar-measured rain data are taken as the input of the hydrological model. The model developed above performs better when radar-measured data, instead of raingauge data, were used in simulating hourly hydrograph at Huangnizhuang station in the Shihe catchment. In addition, the spatial and temporal distributions of state variables, such as soil tension water at any cell within the catchment at any time step, may be obtained by the model.

It should be pointed out that radar-measured data used in this study have been modified according to topographical characteristics and data observed by raingauge stations (Liu *et al.*, 2000). It is true that radar-measured rain data have an advantage of highly spatial and temporal resolutions. However, the greater the distance from the radar station, the lower the accuracy of rain data. It is worth being studied further. An approach to this problem is to build more radar stations, so that the stations can cover the whole study area. When an attempt is made for radar data to be used for the mesoscale or large-scale area, more investment is necessary. In such cases, the equilibrium point between investment and economic loss/risk should be found.

**Acknowledgements** This research was jointly supported financially by the National Natural Science Foundation of China under Grant no. 40171016 and 49794030. The author would like to give thanks to Dr Liu Xiaoyang at Beijing University for providing radar data.

## REFERENCES

- Beven, K. (1989) Changing ideas in hydrology—the case of physically-based models. *J. Hydrol.* **105**, 157–172.
- Doyle, F. J. (1978) Digital terrain models: an overview. *Photogram. Engng & Remote Sens.* **44**(12), 1887–1896.
- Fairfield, J. & Leymarie, P. (1991) Drainage networks from grid digital elevation models. *Water Resour. Res.* **27**(4), 29–61.
- Garbrecht, J. & Campbell, J. (1997) TOPAZ: an automated digital landscape analysis tool for topographic evaluation, drainage identification, watershed segmentation and subcatchment parameterization. *TOPAZ User Manual*, US Dept of Agric.-ARS, Oklahoma, USA.
- Jenson, S. K. & Dominique, J. O. (1988) Extracting topographic structure from digital elevation data for geographical information system analysis. *Photogram. Engng & Remote Sens.* **54**(11), 1593–1600.
- Liu, X. Y., Mao, J. T. & Li, J. R. (2000) Comparison of runoff simulations from radar-estimated rainfall and raingauge measured rainfall in rainfall–runoff model. (Proc. Int. GAME/HUBEX Workshop, GAME/HUBEX Project Office), 147–155. Institute of Low Temperature Science, Hokkaido University, Sapporo, Japan.
- Martz, W. & Garbrecht, J. (1992) Numerical definition of drainage network and subcatchment areas from digital elevation models. *Comp. Geosci.* **18**(6), 747–761.
- Moore, I. D., Grayson, R. B., & Ladson, A. R. (1991) Digital terrain modelling: a review of hydrological, geomorphological and biological applications. *Hydrol. Processes* **5**, 3–30.
- Nash, J. E. & Sutcliffe, J. V. (1970) River flow forecasting through conceptual models, Part I—a discussion of principles. *J. Hydrol.* **10**, 282–290.
- O'Callaghan, F. & Mark, D. M. (1984) The extraction of drainage networks from digital elevation data. *Computer Vision, Graphics & Image Processing* **28**, 323–344.
- Zhao, R. J. (1992) The Xinanjiang model applied in China. *J. Hydrol.* **135**, 371–381.